Journal of Alloys and Compounds 503 (2010) 494–499

Contents lists available at ScienceDirect

Journal of Alloys and Compounds

journal homepage: www.elsevier.com/locate/jallcom

Al–Ni intermetallic composites produced in situ by friction stir processing

Liming Ke[a,*], Chunping Huang[a,b], Li Xing[a], Kehui Huang[a]

[a] National Defence Key Discipline Laboratory of Light Alloy Processing Science and Technology, Nanchang Hangkong University, Nanchang 330063, PR China
[b] State Key Laboratory of Solidification Processing, Northwestern Polytechnical University, Xi'an 710072, PR China

ARTICLE INFO

Article history:
Received 29 December 2009
Received in revised form 5 May 2010
Accepted 7 May 2010
Available online 20 May 2010

Keywords:
Friction stir processing
Intermetallics
Al–Ni composites
Heat treatment

ABSTRACT

Bulk Al–Ni intermetallic composites were synthesized in situ by Friction Stir Processing (FSP) at Al alloy plate with Ni powder. The microstructures and compositions of the composites were analyzed, the hardness and tensile properties of intermetallics were measured. Defect-free composites with Al_3Ni and Al_3Ni_2 intermetallics were successfully produced by FSP and heat treatment. The initial nickel powder present three states after FSP: the coarse nickel aggregation, the sandwich-structure composite and the micron-sized Al_3Ni particles. Typical microstructures of Al_3Ni intermetallics after heat treatment have two microstructures, i.e. the submicron-sized equiaxed crystal when there are fine micron particles uniformly distributed in the aluminum matrix and columnar crystal when Al_3Ni_2 is surrounded. The grain refinement and the precipitation hardening effect of the Al_3Ni intermetallics lead to a significant increase of the microhardness and tensile strength of the Al–Ni composites. The aggregated Ni powders have metallurgy reaction during FSP.

© 2010 Elsevier B.V. All rights reserved.

1. Introduction

Aluminum and its alloys are an important class of materials because of their versatile properties which render them suitable for use in a variety of applications. There has been a constant effort to improve the mechanical properties of Al alloys by various means. Metal matrix composite (MMC) technology is one such method which has become very popular in the past three decades [1]. Aluminum intermetallic compounds are expected to serve as practical materials for their resistance for ware, high hardness and stability at an elevated temperature [2]. However, aluminum intermetallic compounds such as Al_3Ni are so brittle that it alone cannot serve as a structural material. Attempts have been made to compensate the brittleness by embedding it in a ductile matrix material [3–6]. Thus, the advantageous properties can practically be utilized in a structural material and the ductility of matrix material can avoid its brittle shortcoming. In the past few years, various researches have been made to fabricate these Al–Al_3Ni composites by directionally solidification [7], equal-channel angular pressing [8], electromagnetic separation method [9] and mechanical alloying [10].

Friction stir processing (FSP) is a relatively novel multifunctional metal working method, developed based on the basic principles of friction stir welding (FSW) [11]. The severe plastic deformation and material flow in stirred zone can be utilized to achieve bulk alloy modification via mixing of other elements or second phases into the stirred alloys. As a result, the stirred material becomes a metal matrix composite or an intermetallic alloy with much higher hardness and wear resistance. Recently, FSP has been applied successfully to produce Al–Al_2Cu in situ composite from Al–Cu elemental powder mixtures [12], Al–$Al_{13}Fe_4$ in situ nano-composite from Al–Fe elemental powder mixtures [13], Al–Al_3Ti nano-composite from Al–Ti elemental powder blends [14]. During the above three experiments, the alloying elements were pre-mixed with aluminum powders. The pre-mixed alloy powders were cold compacted to 12 mm × 20 mm × 88 mm billet in a steel die set using a pressure of 225 MPa. To improve the billet strength for easier handling in FSP, the green compact was sintered for 20 min at either 773 or 803 K.

In this study, the Ni powders were dispersed in a 1060 Al plate as experimental metal. The experiments were designed to research the feasibility of producing Al–Ni intermetallic composites by FSP and subsequent heat treatment. It does not need other compression and sintering, also reduced powder pre-mixing, simplified the technical process. The distribution of intermetallic in the base metal was observed, and the microhardness and the tensile properties of intermetallic were also examined.

2. Experimental details

The initial materials used are pure aluminum plate (99.6% purity, 5 mm thickness) and pure nickel powder (99.0% purity, 2.3 μm). The as-received nickel powder shows aggregated state before processing in Fig. 1, which makes the uniform dispersion of nickel powder in the matrix difficult. The nickel powder were filled into two rank holes (2.5 mm in diameter and 3 mm in depth) with a interval of 3 mm on two matrix plate before FSP, as shown in Fig. 2. The FSP tool has a columnar shape (Ø 28 mm) with a screw thread probe (M10 mm, 8.5 mm in length). The tool

* Corresponding author. Tel.: +86 791 3863015; fax: +86 791 3953312.
E-mail address: liming_ke@yahoo.cn (L. Ke).

0925-8388/$ – see front matter © 2010 Elsevier B.V. All rights reserved.
doi:10.1016/j.jallcom.2010.05.040

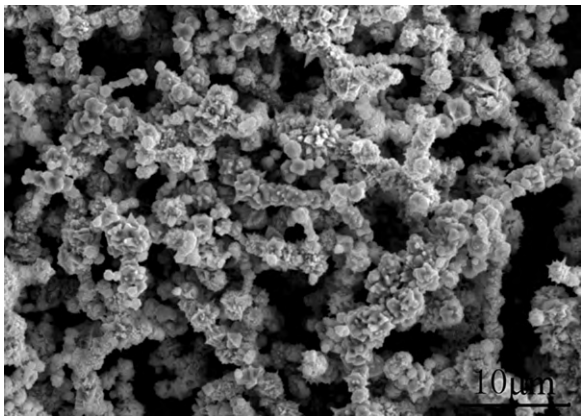

Fig. 1. SEM image of the as-received commercial nickel powder.

penetrated into the plate until the shoulder's head face reached 0.4–0.5 mm under upper surface. The probe was inserted into the interval of two rank holes filled with the nickel powder. The constant tool rotating rate of 1500 rpm and travel speed of 23.5 mm/min were adopted. The tool tilt angle (angle between spindle and work piece normal) of 3° was used. Three FSP passes were applied in order to enhance the Al–Ni reaction. The subsequent heat treatment performed at 550 °C for 6 h after FSP. Transverse sections of the as-produced FSP samples were mounted and then mechanically polished. The distribution of the intermetallic was observed by SEM (FEI QUANTA200), and the microstructure of the etched sample was evaluated by optical microscopy. XRD (BRUKERAXS-D8 ADVANCE, Cu Kα, 40 kV, 40 mA) and EDS (OXFORD 6650) were utilized to identify the phases. The microhardness of different phases was measured using a micro-Vickers hardness tester (HVS-1000) with a load of 50 g for 15 s. Mechanical properties of the composites and 1060Al FSP specimens machined from the stirred zone (SZ) were carried out on an Instron 3382 universal testing machine with an initial strain rate of 1×10^{-3} s^{-1}. The dimensions of the gauge section of tensile specimens were 4 mm in diameter and 22 mm in gauge length. In tensile test, the loading axis was parallel to the traversing direction of FSP.

3. Results and discussion

3.1. Phase composition and microstructure

X-ray diffraction was used to determine the Al–Ni reaction product in situ via FSP and the phase transformation with heat treatment in the FSP samples, as shown in Fig. 3. The only product of the Al–Ni reaction during FSP can be identified as Al_3Ni, as shown in Fig. 3(a). After 3 passes FSP, the nickel peaks still exist, and then disappear and are replaced by Al_3Ni peaks after subsequent heat treatment. More Al_3Ni peaks can be detected from the XRD pattern of heat treatment specimen, and their intensity increased. Two obvious Al_3Ni_2 peaks in the XRD curves with $2\theta = 44–45°$ can be seen for

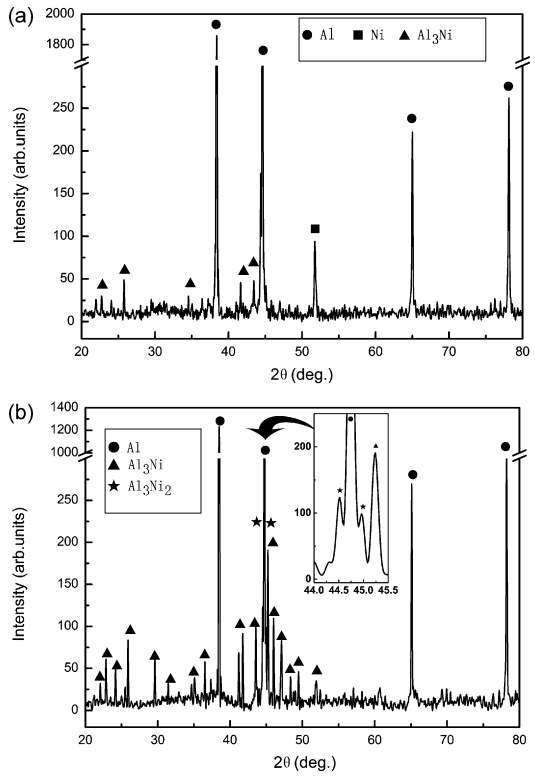

Fig. 3. XRD patterns of Al–Ni composites for: (a) 3 passes FSP and (b) heated at 550 °C for 6 h after FSP.

specimens with heat treatment, as seen in the magnified view of the XRD pattern in Fig. 3(b).

SEM images from the alloying region of FSP and heat treated composites are shown in Fig. 4. No discernible defects were observed. After 3 passes of FSP, the white particle dispersed within the regions was macroscopically well dispersed, as shown in Fig. 4(a). However, the observed clustering particle size is much larger than the initial nickel powder and the shape of the particle is stripped or massive. The fine gray particulates are predominantly spread in this region, which are verified as Al_3Ni by energy dispersive spectroscopy (EDS). The white particles are nickel aggregation, which are dispersed in the Al matrix. The above analyze is consistent with the XRD results. Therefore, Al_3Ni intermetallic was fabricated but nickel powder is not fully reacted with aluminum.

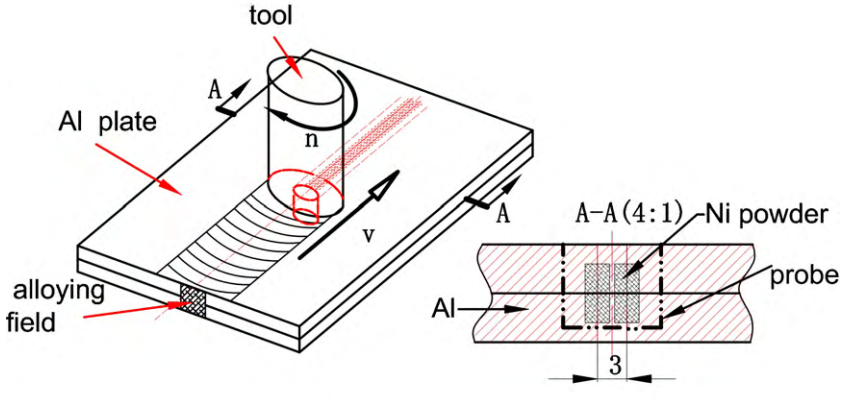

Fig. 2. Schematic diagram of the Al–Ni composites produced by friction stir processing.

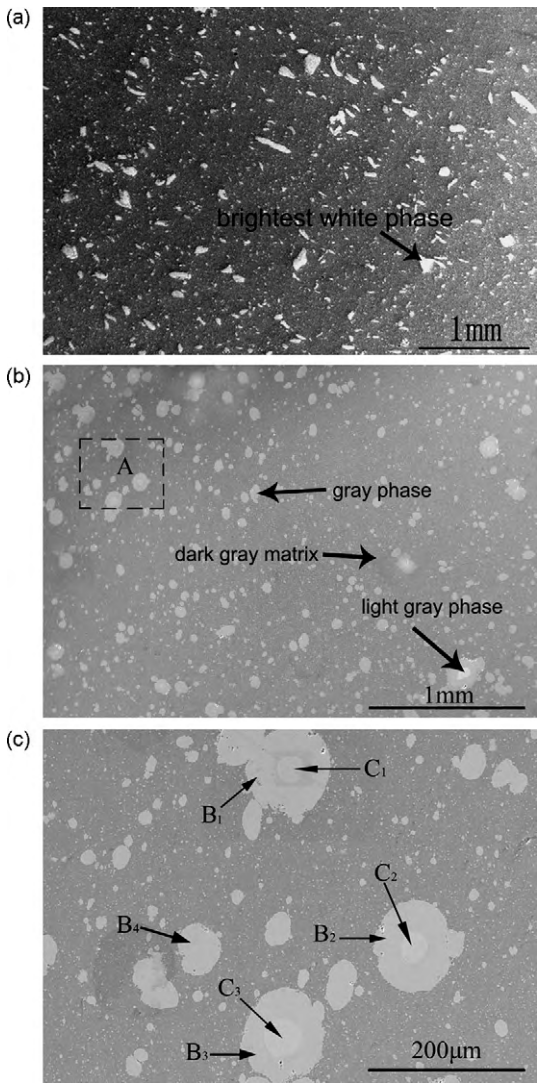

Fig. 4. SEM micrographs showing the particle dispersion: (a) three passes FSP; (b) with subsequent heat treatment at 550 °C for 6 h; (c) the enlarged micrograph of marked A region in (b).

After subsequent heat treatment of the FSP sample at 550 °C for 6 h, the distribution of the gray particles become more uniform in the Al matrix, as shown in Fig. 4(b) and (c). The surfaces of the most particles are smooth. No white particles can be seen from this region. There were just a few regions in which gray material wrapped around the light gray particulates to construct the composite particles, which prove that a wide range of size exists in the particles embedded in the matrix. No evidence of particle fall-out was found. Thus the particles should have better bonding with the matrix.

An SEM equipped with an EDS is also used for the observation of the phase shape and the analysis of its composition after heat treatment. EDS spectrum corresponding to the region marked B_1–B_4 and C_1–C_3 in Fig. 4(c) are shown in Fig. 5. Quantitative results of the average element composition are listed in Table 1. The Al/Ni atom ratio in the region B is in the range of 2.93–3.07, which conclude that the phase is most likely to be Al_3Ni. The phase in the region C is probably Al_3Ni_2, which the Al/Ni atom ratio in the region is in the range of 1.49–1.58. X-ray diffraction was also performed, and the result in Fig. 3 indicates that intermetallic phases Al_3Ni and Al_3Ni_2 exist in the processing zone with subsequent heat treatment. This is consistent with the above EDS analysis.

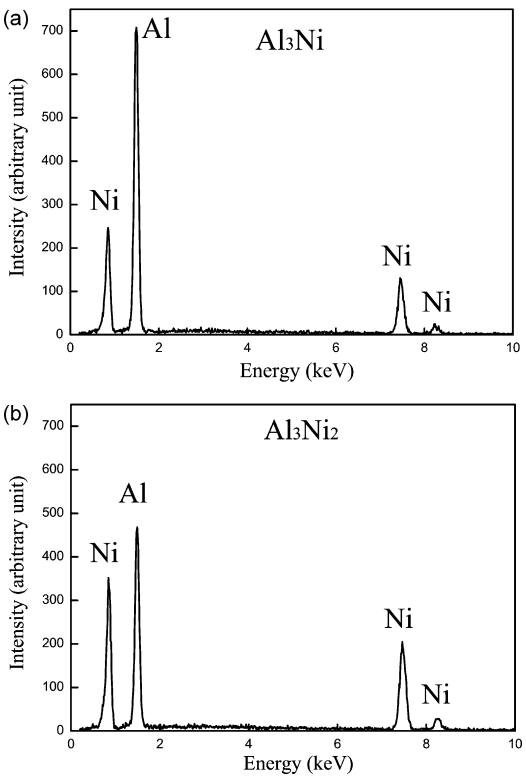

Fig. 5. EDS spectrum corresponding to the region: (a) marked B in Fig. 4(c); (b) marked C in Fig. 4(c).

Up to now, it can be inferred that the brightest white phase is identified as Ni, the dark gray matrix is Al, the light gray phase is Al_3Ni_2, and the gray phase, which surround Al_3Ni_2 particle or dispersed in the Al matrix, is Al_3Ni.

The initial nickel powder aggregated before FSP, as can be seen in Fig. 1. However, it presents three different states after 3 passes FSP as shown in Fig. 6(a). The nickel powders were predominantly cool welding in this regime by the vigorous stirring during FSP at the working temperature around 450 °C and formed a coarse nickel particle, like position A pointed out by the arrow in Fig. 6(a). A gray lamella-structured Al_3Ni surround the coarse nickel aggregation. Fig. 6(b) shows a sandwich structure in region B of Fig. 6(a). The white layer of micron size is nickel and the gray layer is Al_3Ni, which has been verified by EDS. Fig. 6(c) shows some very fine gray particles, which are Al_3Ni particles, uniformly dispersed in the Al matrix. Furthermore, some pits could be observed in Fig. 6(c), which can prove that particles did not get real bonding with base metal and fall off during the preparation of samples.

Typical microstructures of Al_3Ni intermetallics fabricated by 3 passes FSP and subsequent heat treatment are shown in Fig. 7. Obviously, there are fine micron particles distributed uniformly in the aluminum matrix. The Al_3Ni particle with submicron-sized grain dispersed in the matrix aluminum is equiaxed crystal. However, when surround Al_3Ni_2, the grain of Al_3Ni is columnar crystal. Due to severe deformation and short time at elevated temperature in

Table 1
The average chemical compositions of different regions corresponding to Fig. 5 analyzed by EDS (at.%).

Elements	B_1	B_2	B_3	B_4	C_1	C_2	C_3
Al	75.01	74.93	75.44	74.55	61.28	59.82	61.02
Ni	24.99	25.07	24.56	25.45	38.72	40.18	39.92
Al/Ni	3.0	2.99	3.07	2.93	1.58	1.49	1.53

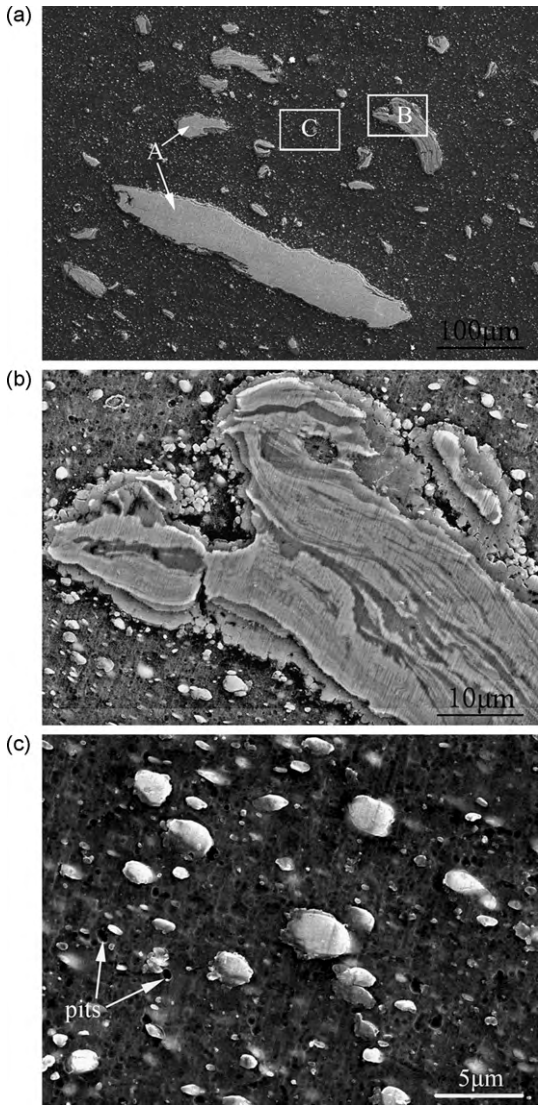

Fig. 6. The microstructure of FSP specimen by SEM: (a) as-FSP condition; (b) the enlarged micrograph of the marked B region in (a); (c) the enlarged micrograph of marked C region in (a).

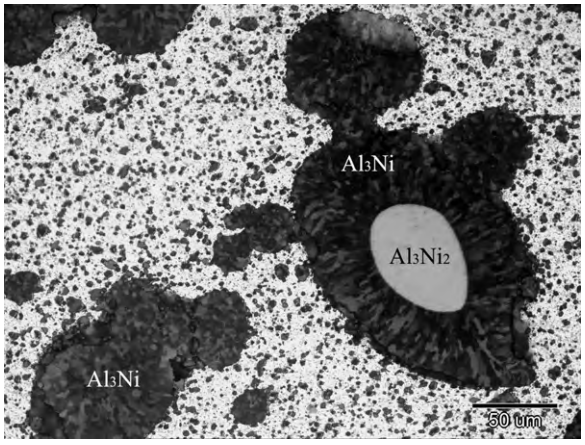

Fig. 7. Optical microscope image of Al_3Ni grain.

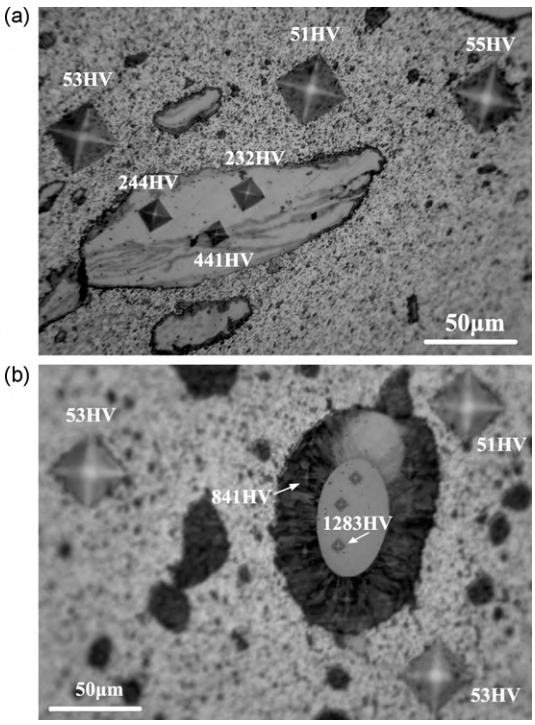

Fig. 8. Optical microscope images of indentation prints: (a) FSP specimen; (b) heat treatment specimen.

FSP, grain growth was limited effectively in Al–Al_3Ni intermetallic composites.

3.2. Hardness measurement and tensile properties

Fig. 8 shows the indentation prints marked by the microhardness test under a load of 50 g and a dwell time of 15 s. The optical micrographs were obtained at the same magnification in order to compare the size of the indentation prints. For Al–Ni after 3 passes FSP, as shown in Fig. 8(a), the average microhardness of the Al matrix and nickel particles were 53 and 238 HV, respectively. At the sandwich-structure region consisting of nickel and Al_3Ni, the value of microhardness is 441 HV. The microhardness of nickel particles is lower than that of the pure nickel after equal-channel angular pressing slightly, which is approximately 250 HV in the Ref. [15]. It can be proved that the initial nickel powders have metallurgy reaction.

On the other hand, the indentation prints of the Al_3Ni and Al_3Ni_2 intermetallic are obviously smaller than that of the Al matrix and nickel phases, as shown in Fig. 8(b). The microhardness for the Al_3Ni_2 and Al_3Ni intermetallics were measured as 1283 HV and 841 HV respectively, and the Al matrix was 52 HV for the sample heat treated by 550 °C for 6 h. In addition, the maximum microhardness for samples fabricated by FSP without nickel powder was 37 HV. It is suggested that the grain refinement and the precipitation hardening effect of the Al_3Ni intermetallics resulted in the significant increase of the microhardness for the Al–Al_3Ni composites.

The tensile stress–strain curves of composite and 1060Al FSP specimens are shown in Fig. 9, which presents that the Al–Al_3Ni composite has an average 0.2% yield stress of 110 MPa, an ultimate strength about 144 MPa, and a failure strain greater than 0.2. The ultimate strength of composite specimen is much higher than that of 1060Al FSP (84 MPa). The significant improvement of the tensile strength can be attributed to the presence of large amount of Al_3Ni in the composite.

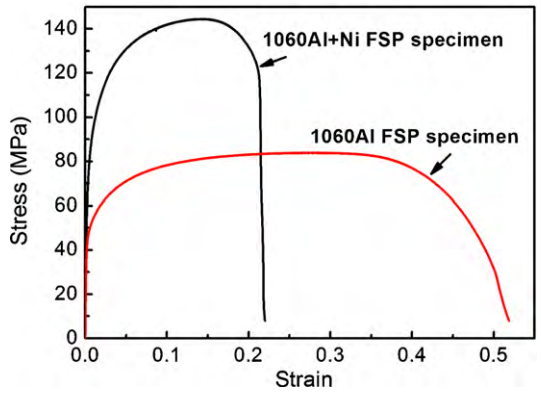

Fig. 9. Tensile stress–strain curves for FSP specimens machined from Al–Ni composites and 1060Al.

3.3. Reaction mechanism

The intense plastic deformation around the tool and the friction between tool and workpiece contribute to the heat increase in the stirred zone during FSP. Localized heating increase the local temperature of the material to the range in which it can be plastically deformed easily. The maximum temperature in the stirred zone during FSP of various aluminum alloys is found to be between $0.6T_m$ and $0.9T_m$, which depends on the ratio of rotation rate to translation speed [11]. In this experiment, the maximum temperature is about 450 °C. Therefore, it is suggested that FSP can provide severe plastic strain [11,16], which not only promotes mixing, but also increases the diffusion rate of elements, thereby accelerates the reaction between Al and Ni; Otherwise, FSP can also provide elevated temperature to facilitate the formation of intermetallic phase in situ and accelerate the reaction of Al and Ni to form Al_3Ni particles.

Based on the Ni–Al phase diagram shown in Fig. 10, the binary system exhibits two solid solutions and five stable intermetallic compounds, i.e., Al3Ni, Al3Ni2, NiAl, Ni5Al3 and Ni3Al, two of which have been detected in this study. Gasparyan and Shteinberg [17] used a specially designed DTA to show the evidence of precombustion solid-state reactions, eutectic melting and proposed three reaction steps producing Al_3Ni, Al_3Ni_2 and NiAl successively. The phase formation sequence was described as following equation:

$$3Al + Ni \rightarrow NiAl_3 + 258\,kcal/mol \quad (1)$$

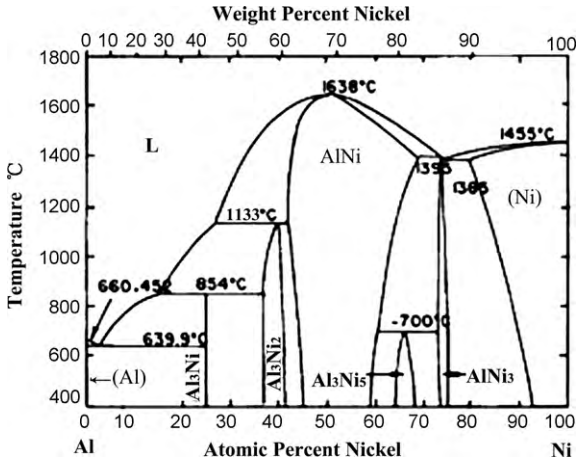

Fig. 10. Binary phase diagram of Al–Ni system. Taken from Ref. [18].

$$NiAl_3 + Ni \rightarrow Ni_2Al_3 + 90\,kcal/mol \quad (2)$$

$$Ni_2Al_3 + Ni \rightarrow 3NiAl + 212\,kcal/mol \quad (3)$$

During the FSP of Al–Ni compounds, Ni spherical particles were surrounded by continuous Al matrix. Al are easily deformed and wrapped around the Ni particulates to construct the composite particles. The reaction between Al and Ni is exothermic, in which a $NiAl_3$ phase grows at the Ni–Al interface as a spherical shell according to Eq. (1). The heat provided by friction stir of the rotating tool can initiate the exothermic reaction. The large plastic strain in FSP can shear the metal powders and break the oxide film surrounding Ni particles, which causes intimate contact between Al and Ni and promotes the reaction. At low temperature, Al is the fastest diffusing species in the Ni/Al diffusion couples [19]. Therefore, $NiAl_3$ grows via the diffusion of Al to the Ni phase at Al/Ni interface. When the nickel powder is not aggregated, it formed Al_3Ni particles directly and then dispersed in the matrix following the metal flow of FSP, as can be seen in Fig. 6(c). On the contrary, when the nickel powder is aggregated, coarse nickel particles are formed. Because the diffusion length of Al away from the interface is limited in a short time, only thin films of Al_3Ni intermetallics have been produced in the outer layer of the coarse nickel particles. Some Al_3Ni wrapped around the nickel particulates to construct the composite particles of Al_3Ni/Ni, as seen in Fig. 6(a). As a result of multi-passes FSP stirring, a sandwich-structure composite of Al/Al_3Ni/Ni has been fabricated, as shown in Fig. 6(b).

With the subsequent heat treatment at 550 °C for 6 h after FSP, NiAl3 grows via the diffusion of Al through the NiAl3 phase to the NiAl3/Ni interface initially. After all the diffused Al has been consumed, Ni_2Al_3 starts to grow at the Ni–$NiAl_3$ interface according to Eq. (2). When Ni is consumed, the reaction rate decreases so that even after the temperature is raised, a two-layer Ni2Al3/$NiAl_3$ structure is remained as shown in Figs. 4(c) and 7. A similar structure was also observed by Faber et al. in their studies of the reaction processes in Ni–Al diffusion couples and Ni–Al powders [20,21].

The released heat due to the exothermic reaction of Al_3Ni and Al_3Ni_2 maybe cause melting of eutectic Al and Al_3Ni. Otherwise, a great gradient of temperature forms between the interfaces of Al/Al_3Ni and Al_3Ni/Al_3Ni_2. It is believed that the evolution of the columnar crystal of Al_3Ni microstructure is caused by the large gradient of temperature. The eutectic melting solidified rapidly because of the quickly dissipated heat from the surrounding aluminum matrix.

4. Conclusions

The finding in this work can be summarized as follows:

(1) Defect-free Al–Ni intermetallic composites were successfully produced by 3 passes FSP and with a subsequent heat treatment at 550 °C for 6 h. Al_3Ni and Al_3Ni_2 exist in the processing zone, and the particles were found to have good bonding with the matrix.
(2) The initial nickel powder present three different states after 3 passes FSP: the coarse nickel aggregation surrounded by a gray lamella-structured Al_3Ni, a sandwich-structure composite with Al_3Ni and nickel layers and micron-sized Al_3Ni particles uniformly dispersed in the Al matrix.
(3) Typical microstructures of Al_3Ni intermetallics which fabricate by FSP and heat treatment are: the submicron-sized equiaxed crystal when there are fine micron particles uniformly distributed in the aluminum matrix and the columnar crystal when surround Al_3Ni_2.
(4) After 3 passes FSP, the grain refinement and the precipitation hardening effect of the Al_3Ni intermetallics resulted in the sig-

nificant increase of the microhardness and tensile strength for the Al–Al_3Ni composites. The aggregated Ni powders have metallurgy reaction during FSP. The microhardness for the Al_3Ni_2 and Al_3Ni intermetallics were measured as 1283 and 841 HV respectively. The ultimate strength of composite is 144 Mpa, which is 171% of the 1060Al FSP.

Acknowledgments

This research was supported by the National Natural Science Foundation of China under grant no. 50674056. The authors thank Dr. W. Yang and Dr. H.F. Wang for useful discussion.

References

[1] D. Yadav, R. Bauri, Mater. Lett. 64 (2010) 664–667.
[2] T.P.D. Rajan, R.M. Pillai, B.C. Pai, J. Alloys Compd. 453 (2008) L4–L7.
[3] Y. Fukui, K. Takashima, C.B. Ponton, J. Mater. Sci. 29 (1994) 2281–2288.
[4] Y. Fukui, H. Okada, N. Kumazawa, Y. Watanabe, Metall. Mater. Trans. A 31 (2000) 2627–2636.
[5] J.B. Fogagnolo, E.M.J.A. Pallone, D.R. Martin, C.S. Kiminami, C. Bolfarini, W.J. Botta, J. Alloys Compd. 471 (2009) 448–452.
[6] B.S.B. Reddy, K. Rajasekhar, M. Venu, J.J.S. Dilip, Siddlhartha Das, Karabi Das, J. Alloys Compd. 465 (2008) 97–105.
[7] J.Y. Uan, L.H. Chen, T.S. Lui, Acta Mater. 49 (2001) 313–320.
[8] Z.G. Zhang, E. Akiyama, Y. Watanabe, Y. Katada, K. Tsuzaki, Corrosion Sci. 49 (2007) 2962–2972.
[9] C.J. Song, Z.M. Xu, J.G. Li, Mater. Sci. Eng. A 445–446 (2007) 148–154.
[10] G. Gonzalez, A. Sagarzazu, D. Bonyuet, L.D. Angelo, R. Villalba, J. Alloys Compd. 483 (2009) 289–297.
[11] R.S. Mishra, Z.Y. Ma, Mater. Sci. Eng. R 50 (2005) 1–78.
[12] C.J. Hsu, P.W. Kao, N.J. Ho, Scripta Mater. 53 (2005) 341–345.
[13] I.S. Lee, P.W. Kao, N.J. Ho, Intermetallics 16 (2008) 1104–1108.
[14] C.J. Hsu, C.Y. Chang, P.W. Kao, N.J. Ho, C.P. Chang, Acta Mater. 54 (2006) 5241–5249.
[15] K. Neishi, Z. Horita, T.G. Langdon, Mater. Sci. Eng. A 325 (2002) 54–58.
[16] E.A. El-Danaf, M.M. El-Rayes, M.S. Soliman, Mater. Des. 31 (2010) 1231–1236.
[17] A. Gasparyan, A. Shteinberg, Combus. Explos. Shock Waves. 24 (1988) 324–330.
[18] H. Baker, H. Okamoto, ASM Handbook. Vol.3: Alloy Phase Diagrams, ASM International, Materials Park, Ohio, USA, 1992.
[19] E. Ma, M.A. Nicolet, M. Nathan, J. Appl. Phys. 65 (1989) 2703–2710.
[20] L. Farber, I. Gotman, E.Y. Gutmanas, A. Lawley, Mater. Sci. Eng. A 244 (1998) 97–102.
[21] L. Farber, I. Gotman, E.Y. Gutmanas, Mater. Lett. 34 (1998) 226–231.